AN EXPERIMENTAL STUDY OF A WAKE-BOUNDARY INTERACTION

V. BASKARAN† and P. BRADSHAW‡

Department of Aeronautics,
Imperial College of Science and Technology
London SW7 2BY
ENGLAND

ABSTRACT

Mean flow and turbulence measurements were conducted in a flat plate turbulent boundary layer merging with the wake of a circular cylinder inclined in the cross-stream plane, simulating the wake of an axial turbomachine turbine blade interacting with the boundary layer on a downstream blade. Experiments were conducted for angles of inclination of the wake, with respect to the plane of the flat plate, of 0°, 10° and 20°. The results demonstrate that the primary effect of the interaction is simply to reduce the skin friction due to the reduced velocity in the wake of the cylinder. The wake is bodily shifted towards the local free stream by the growing boundary layer. The turbulence of the wake, regarded as "free stream turbulence", appears to have little effect on skin friction on the flat plate. Pressure gradients on the plate would not alter these conclusions qualitatively.

INTRODUCTION

One of the major problems in turbomachinery flows is the prediction of the interaction of the wake of one blade with the boundary layer on a blade in the next row downstream. In this study we investigate an idealised version, in which a circular cylinder wake interacts with a flat plate boundary layer, the cylinder being inclined to the plate in front view so as to represent the practically important case of twisted or non-radial blades. As far as we are aware, this flow has not been investigated previously, although several experiments have been done with turbulence generators consisting of translating rows of parallel rods, simulating the movement of a rotor relative to a stator. These studies all report increases in skin friction or aerofoil drag, attributed to the "free-stream turbulence" caused by the rods. The present work also differs from earlier studies on interaction between circular cylinder wakes and boundary layers (see for example Marumo et al. 1978) in that the circular cylinder was positioned well upstream of the leading edge of the flat plate on which the boundary layer grew, whereas in the earlier investigations the cylinder was downstream of the leading edge, representing multi-element aerofoils rather than turbomachine blades.

In many axial turbomachine compressors and turbines, the wake of one blade meets the span of a downstream blade at an angle: even the leading edge and trailing edge of a single blade are in general not parallel or radial, due to blade twist. As a consequence, skin friction and surface heat transfer rates, and hence the overall performance of the turbomachine, are expected to be affected in a more complicated way than if the blades were parallel.

This work also has some relevance to the influence of free stream turbulence on turbulent boundary layers, the free stream turbulence being generated by the wake of the cylinder rather than by screens or grids: for a review of grid-turbulence effects, and some recent results, see Baskaran et al. (1989). The effect of nearly-isotropic, unsheared grid-generated free-stream turbulence is to increase the skin-friction coefficient and the surface heat transfer rates. In contrast, the results of the present study show that skin friction coefficient and surface heat transfer rate actually decrease. That is, the main effect is that the drag of an upstream body leads to a velocity defect in its wake, and the skin friction on a downstream body is reduced accordingly. The effect of the wake turbulence seems secondary.

APPARATUS AND TECHNIQUES

The experiments were conducted in the 910 mm × 910 mm low-speed wind tunnel in the Department of Aeronautics. The experimental arrangement is shown in figure 1. The flat plate used in the present study is the same as that used by Hancock & Bradshaw (1983). A ogival-profile nose piece with sharp leading edge was used

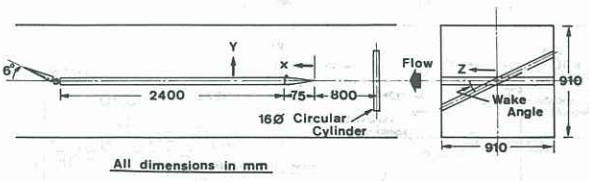

Figure 1. Experimental arrangement.

to avoid intermittent leading-edge separation due to the random normal-component velocity fluctuations in the wake. Nominally-zero streamwise pressure gradient was achieved using a flap to locate the front stagnation point at the sharp leading edge. A 1.2 mm trip wire glued at 80 mm from the leading edge was used to promote transition. A 16 mm diameter circular cylinder was mounted 0.8 m (50 diameters) ahead of the plate, spanning the test section. The circular cylinder could be held with its axis at an angle to the span of the flat plate (figure 1). We refer to this angle as the 'wake angle' for brevity. The cylinder

† Aeronautical Research Laboratories, DSTO, Salisbury, Australia.

‡ Thermosciences Division, Mechanical Engineering Dept., Stanford University, Stanford, CA 94305, USA.

axis intersected the plane of the flat plate on the tunnel centre line, z = 0 in the graphs below. Experiments were performed for three wake angles, viz. 0°, 10° and 20°, at a tunnel velocity of 16 m/s.

The measurements included skin-friction coefficients, mean velocity profiles and those turbulence quantities that appear in the transport equations for the Reynolds stress components. Skin-friction coefficients were measured using a 1.1 mm diameter Preston tube, giving good agreement with those inferred from the law of the wall with constants 5.62 and 5.2. Mean velocity profiles in the boundary layer were measured on-line using a traverse gear controlled by a BBC Micro computer and carrying a 1.1 mm pitot tube.

Turbulence measurements were made using crossed hot-wire probes. The probes were home made with platinum core Wollaston wire of 5μm diameter, soft soldered to the prongs and etched to give an active length of about 1.2 mm. Melbourne University type constant-temperature anemometers were used, with a fixed resistance ratio of 1.8. The wires were statically calibrated in the local free stream before and after every profile. Yaw calibration results were fitted to a cosine cooling law to give the effective wire angles. The correlations between v and w fluctuations were obtained by rolling the probe about its axis into ±45° planes, so that the wires responded to $(v \pm w)/\sqrt{2}$. The cross stream component of turbulent shear stress, $-\overline{vw}$, and the associated triple products, viz. $\overline{v^2 w}$, $\overline{vw^2}$ and $\overline{uvw}$, were deduced as the sums and differences of mean squares and mean cubes measured in these two planes. Some selected fourth order quantities were also obtained. All turbulence measurements were obtained on-line using a sample/hold unit, a Tecmar/Labmaster 12 bit analog-to-digital converter and an IBM-PC "portable" micro-computer programmed in Microsoft Fortran. 20,000 samples per wire per roll plane were collected at each point in the boundary layer at a sampling frequency of 200 Hz.

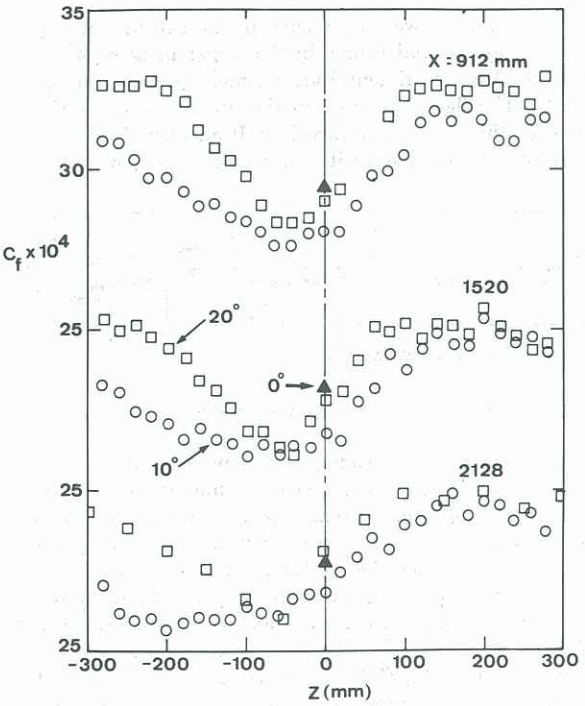

Figure 2. Spanwise skin friction distributions.

RESULTS

Figure 2 shows the spanwise skin-friction distributions at different streamwise locations for different wake angles. The distributions follow the expected trend in that the boundary layer on one half of the surface ($z < 0$, the right half as seen looking downstream in figure 1) interacts with the wake, while the other side of the wake affects the boundary layer less since it passes under the plate. At large distances from the centre line – at least on the "unaffected" side – the C_f distribution asymptotes to the two-dimensional boundary layer value. The skin friction coefficient for the 10° wake angle decreases more than that for the 20° wake angle on the affected side, and the extent of the minimum increases as the flow proceeds downstream. This may be due to more complete merging of the wake with the boundary layer in the 10° case.

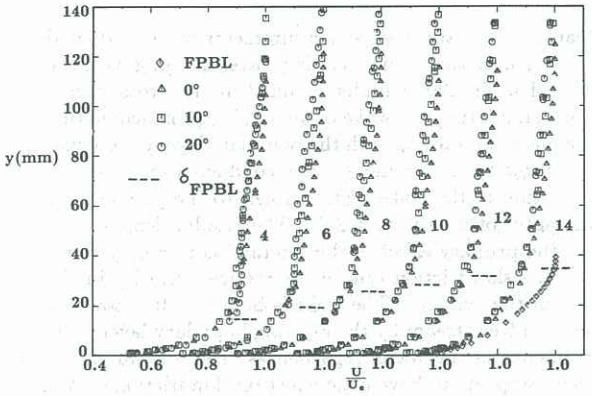

Figure 3. Mean velocity profiles along $z = -80$ mm.

Figure 3 shows the mean velocity profiles measured in the plane z = - 80 mm, roughly at the position of minimum C_f (figure 2). The streamwise distance of the profiles from the leading edge in meters is given as

$$x = 0.152 \times (\text{station number}) \qquad (1)$$

The station numbers are shown on figure 3 and later figures showing profiles. The flat-plate profile at station 14 in the absence of the cylinder (diamond symbols in figure 3) demonstrates how the outer region of the boundary layer changes when the wake is present. In fact, the reduction in skin friction drag, even at 0° wake angle, can be qualitatively attributed to the reduced mean velocity seen by the undisturbed boundary layer without invoking any turbulence mechanism as such: there is certainly no hint that the cylinder acts as a large-eddy break-up device. The profiles at small x retain the velocity minimum found in the undisturbed cylinder wake, but the profiles become monotonic at large x. The shape factor, H changes from an undisturbed value of 1.42 to 1.26 at 0° wake angle due to the modification of the outer layer. Variation in the wake angle does not affect the value of H much in the region of strong interaction.

The downstream growth of the boundary layer and displacement thicknesses corresponding to different wake angles are compared to those in the absence of the cylinder in figure 4, together with the growth of the half-width of the wake of an isolated circular cylinder, as calculated from the formula given in Schlichting (1968),

$$b_{1/2} = 0.25\sqrt{xC_D d} \qquad (2)$$

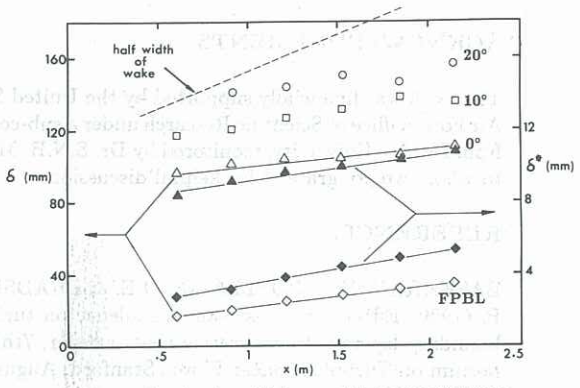

Figure 4. Boundary layer thickness and displacement thickness along $z = -80$ mm.

The drag coefficient of the cylinder was inferred from a graph of C_D versus Reynolds number based on the diameter, Re_d, given in Schlichting (1968). The value of Re_d in the present experiment is 1.7×10^4. The decrease in the wake growth rate in the presence of the flat plate is expected, since the latter acts like a splitter plate. The identical growth rates of the displacement thickness, $d\delta^*/dx$, in the cases of 0° wake angle and the undisturbed boundary layer demonstrates that the wake is bodily shifted by the growing boundary layer towards the local free stream. Further changes in displacement thickness and boundary layer thickness for the other two wake angles are only marginal.

The profiles of the normal-stress components, $\overline{u^2}/U_e^2$, $\overline{v^2}/U_e^2$, $\overline{w^2}/U_e^2$, and the shear stress component, $-\overline{uv}/U_e^2$, are shown for $z = -80$ mm in figure 5 and 6, for the different wake angles as well as for the undisturbed boundary layer. The wall shear stress is also shown in figure 6. The profiles of the stress components show spectacular differences for different wake angles, but these can be explained qualitatively by superposition of the boundary-layer stress profiles and the corresponding stress distribution across the undisturbed cylinder wake. Note for instance the stress maximum in the outer region ($y/\delta > 0.2$), especially for the shear stress profile: this maximum decays as the flow proceeds downstream. All the outer region profiles neatly blend into the distributions in the undisturbed boundary layer. The profiles corresponding to the 20° wake angle also demonstrate clearly the bodily shift of wake fluid by the growing boundary layer, as indicated by the upward propagation of the maximum of the shear stress profile almost at the same rate as the undisturbed boundary layer thickness, as marked in the figure. The profiles of all the stress components, except the longitudinal normal stress $\overline{u^2}/U_e^2$, tend to cluster just outside the inner region, regardless of the wake angle: this suggests that the large stress changes in the outer layer have a comparatively weak influence on the shear stress near the wall and hence on the skin friction.

Figure 7 shows the spanwise distribution of shear stress, $-\overline{uv}$, non-dimensionalised by the edge velocity, U_e, at a fixed distance from the wall of $y = 10$ mm at station 10 ($x = 1520$ mm). Note that $y = 10$ mm is well outside the constant-stress region (inner or logarithmic region), so that the shear stress is not expected to vary in phase with the skin friction distribution (figure 2). However, as for the skin friction distribution, most of the effect of the wake ocurs on the negative-z side. The distribution corresponding to zero wake angle is nearly two-dimensional, as it should be, while the shear stress profiles for the other two

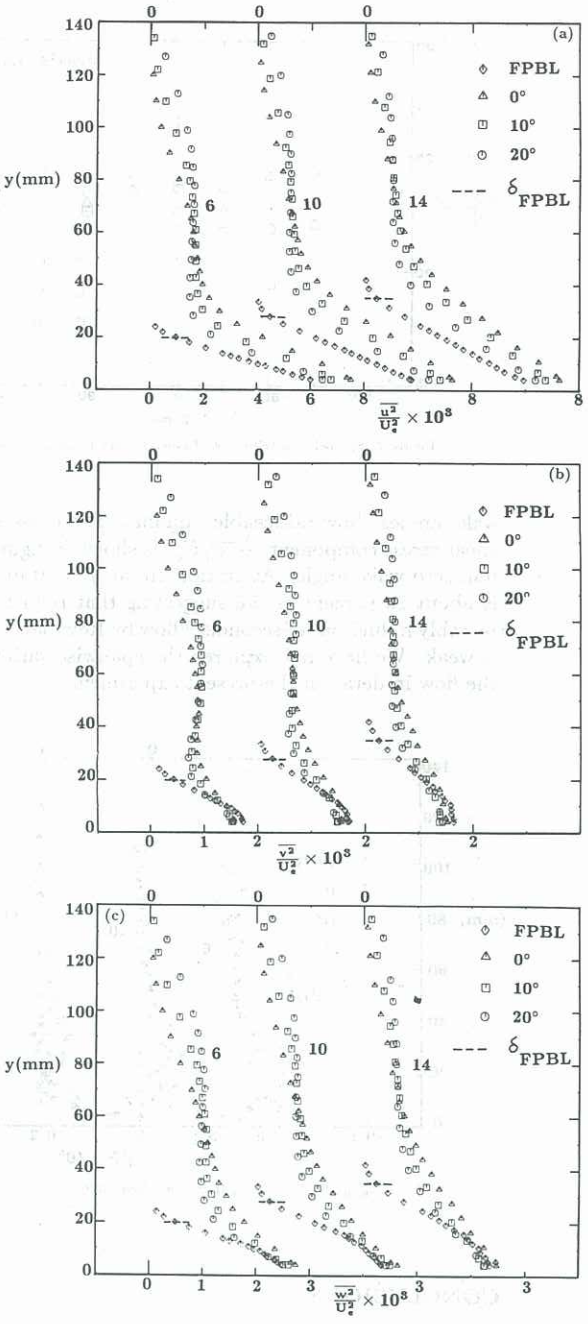

Figure 5. Profiles of Reynolds normal stress components. (a) $\overline{u^2}/U_e^2$ (b) $\overline{v^2}/U_e^2$ (c) $\overline{w^2}/U_e^2$

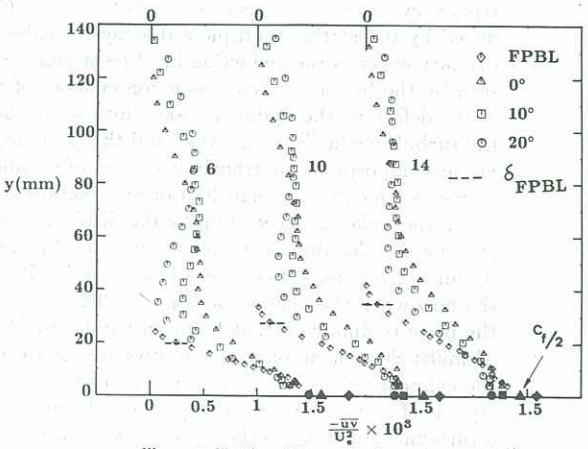

Figure 6. Profiles of Reynolds shear stress, $-\overline{uv}/U_e^2$.

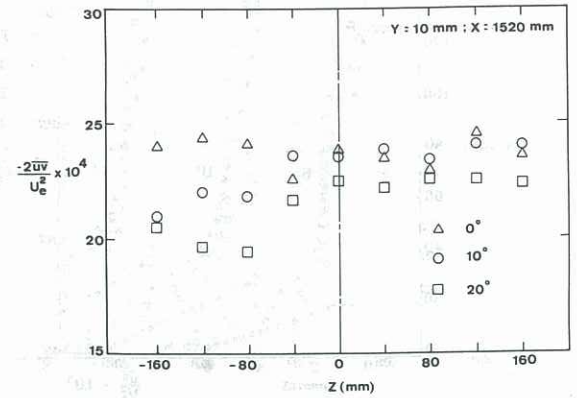

Figure 7. Spanwise distribution of twice Reynolds shear stress, $-2\overline{uv}/U_e^2$.

wake angles show noticeable minima. The cross stream shear stress component, $-\overline{vw}/U_e^2$, is shown in figure 8 for non-zero wake angle. At station 10, at $y = 10$ mm, $-\overline{vw}$ is about 10 percent of $-\overline{uv}$ suggesting that reduction (or possibly induction) of secondary flow by Reynolds stresses is weak. We have not explored the spanwise variation of the flow in detail in the present experiment.

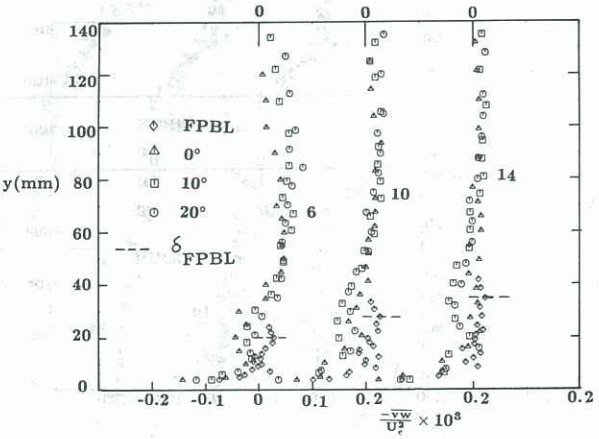

Figure 8. Profiles of Reynolds shear stress, $-\overline{vw}/U_e^2$.

CONCLUSIONS

The skin friction in a turbulent boundary layer on a flat plate decreases in the presence of the wake of a fixed upstream cylinder, in contrast to the increase in C_f produced by translating multiple-rod arrays. Evidently the primary effect is the reduction in "free stream" velocity seen by the boundary layer, as a consequence of the velocity defect in the cylinder wake: interaction between the turbulence fields of the wake and the boundary layer are less important. (A translating array of parallel rods increases time-average skin friction because the flow between the wakes is speeded up by the displacement effect of the wakes, leading to an increase in mean-square velocity for a given mass flow rate.) The general behaviour of the flow when the cylinder axis is parallel to the span of the plate is similar to that found in various idealizations of multi-element aerofoils. The flow in the case where the cylinder axis is inclined to the plane of the boundary layer is of more interest as it represents the interaction of a turbomachine blade wake with the boundary layer on a following non-radial blade.

ACKNOWLEDGEMENTS

The work was financially supported by the United States Air Force Office of Scientific Research under a sub-contract from Purdue University, monitored by Dr. S.N.B. Murthy to whom we are grateful for helpful discussions.

REFERENCES

BASKARAN, V., ABDELLATIF, O.E. & BRADSHAW, P. (1989) Effects of free-stream turbulence on turbulent boundary layers with convective heat transfer, 7th Symposium on Turbulent Shear Flows, Stanford, August.

HANCOCK, P.E. & BRADSHAW, P. (1983) The effect of free stream turbulence on turbulent boundary layers, J. Fluids Engg., 105, pp. 284-289.

MARUMO, E., SUZUKI, K. & SATO, T. (1978) A turbulent boundary layer disturbed by a cylinder, J. Fluid Mech., 87, pp. 121-141.

SCHLICHTING, H. (1968) Boundary-Layer Theory. Sixth Edition, McGraw-Hill Book Company, New York.

NOMENCLATURE

$b_{1/2}$ – half width of the circular cylinder wake

C_f – local skin friction coefficient, $\tau_w/(1/2\rho U_e^2)$

C_D – drag coefficient of the circular cylinder

d – diameter of the circular cylinder

Re_d – Reynolds number based on the cylinder diameter, $U_e d/\nu$

U_e – local free stream mean velocity

$\overline{u^2}, \overline{v^2}, \overline{w^2}$ – Reynolds normal stress components

$-\overline{uv}$ – streamwise Reynolds shear stress

$-\overline{vw}$ – cross stream Reynolds shear stress

x – streamwise distance from the plate leading edge

y – distance normal to the wall

z – spanwise distance from the centre line

δ – boundary layer thickness, $y = \delta$ where $U/U_e = 0.995$

δ^* – momentum thickness of the boundary layer